Trapped-Ion State Detection through Coherent Motion

D. B. Hume,* C. W. Chou, D. R. Leibrandt, M. J. Thorpe, D. J. Wineland, and T. Rosenband
Time and Frequency Division, National Institute of Standards and Technology, Boulder, Colorado 80305

Quantum-limited experiments with trapped atomic ions rely on sensitive methods of detecting an ion's state. Current detection techniques are applicable only to relatively simple systems, which precludes most atomic and molecular species. Here, we demonstrate a technique that can be applied to a larger class of ion systems. We couple a "spectroscopy" ion ($^{27}Al^+$) to a "control" ion ($^{25}Mg^+$) in the same trap and perform state detection through off-resonant laser excitation of the spectroscopy ion that induces coherent motion. The motional amplitude, dependent on the spectroscopy ion state, is measured either by time-resolved photon counting, or by resolved sideband excitations. The first method provides a simplified way to distinguish "clock" states in $^{27}Al^+$, which avoids ground state cooling and sideband transitions. The second method reduces spontaneous emission and optical pumping on the spectroscopy ion, which we demonstrate by nondestructively distinguishing Zeeman sublevels in the $^1S_0$ ground state of $^{27}Al^+$.

Experiments on individual quantum systems face the challenge of isolating the system from the environment while making it accessible to external measurement and control. One way this conflict appears is during state detection when small energy differences between quantum states are amplified into directly measurable signals. According to quantum theory, projective measurement leaves the system in its observed eigenstate, sometimes called a quantum nondemolition or nondestructive measurement. However, unwanted perturbations to the quantum state make this ideal difficult to achieve experimentally, and near-perfect projective measurements, characterized by occasional "quantum jumps" between discrete signal levels, have been realized in only a few physical systems [1–5].

In the case of a trapped atom, transitions between two atomic eigenstates can act as a switch for resonant photon scattering, which is observed with a photon counter [1]. This "electron shelving" technique is a standard tool in atomic physics, but its application is limited to systems where optical pumping does not disrupt the state being measured. Recently developed techniques indirectly detect the state of one or more "spectroscopy" ions by coupling them to a "control" ion of a different species [6, 7]. Indirect detection begins by cooling the ions close to the ground state. Subsequent resolved-sideband transitions implement a quantum gate between the spectroscopy ion and the control ion whose state is then detected. Two drawbacks of this technique are that it relies on ground state cooling, which adds significant experimental complication, and it requires narrow optical resonances, which limit it to relatively few atomic systems.

Here, we demonstrate an indirect detection technique that does not rely on photon scattering [8] or sideband transitions on the spectroscopy ion, making it suitable for a larger class of atomic and molecular systems. As with previous indirect detection techniques we use laser excitation on the spectroscopy ion to induce state-dependent motion that is detected using the control ion. However, here, we consider only off-resonant interactions with the spectroscopy ion through a Stark shift $S^{(\mathrm{i})}$ that depends on the state $|i\rangle$. Spatial variation in this Stark shift (i.e. due to an intensity or polarization gradient) gives rise to an optical dipole force, $\boldsymbol{F}^{(\mathrm{i})}(\boldsymbol{z},t) = -\boldsymbol{\nabla} S^{(\mathrm{i})}$, which can be sensitively detected when it is modulated at the frequency ω_M of a normal mode of motion [9–11]. During this optical drive the spectroscopy ion behaves like a classical driven harmonic oscillator with resonant driving force, $\boldsymbol{F}^{(\mathrm{i})}(t) = \boldsymbol{F}_0^{(\mathrm{i})} \cos(\omega_M t + \phi_M)$, where $\boldsymbol{F}_0^{(\mathrm{i})}$ is the oscillation amplitude of the Stark–shift gradient at the ion position, and ϕ_M is its phase. Through resonant enhancement, forces of 5 yN ($\mathrm{yN} = 1 \times 10^{-24}$ N) have been detected [12], equivalent to a Stark shift gradient of approximately 7.5 kHz over 1 μm. This high sensitivity can be exploited for state detection by utilizing far off-resonant interactions with the spectroscopy ion that result in low probability of a state transition from photon scattering.

Our experiment, sketched in Fig. 1(a), confines a $^{25}Mg^+$ ion and a $^{27}Al^+$ ion along the axis ($\hat{\boldsymbol{z}}$) of a linear Paul trap whose normal mode frequencies for a single Mg^+ ion are $\{\omega_x, \omega_y, \omega_z\} = 2\pi \times \{5.1, 6.8, 3.0\}$ MHz. For the pair Mg-Al, this corresponds to an axial in-phase (COM) mode frequency of $\omega_M = 2\pi \times 2.94$ MHz with ground-state amplitudes $z_{0,\mathrm{Mg}} = 5.64$ nm and $z_{0,\mathrm{Al}} = 5.86$ nm. The dipole force is produced by two σ^+-polarized, counter–propagating laser beams detuned from the $^1S_0 \rightarrow {}^3P_1$ transition (linewidth $\Gamma/2\pi = 520$ Hz) [13] in Al^+ by $\Delta_R/2\pi \simeq 20$ MHz. The interference of these two beams produces a "walking" wave intensity pattern [9] at the Al^+ ion. The resulting optical dipole force is modulated at the lasers' difference frequency, $\Delta\omega = \omega_M$. Because the force must be coherent with the ion motion during the integration time, we measure $\Delta\phi$ in an interferometer near the trap and stabilize it with an acousto-optic modulator in one of the beam paths, observing a relative coherence time at the position of the ions of about 200 s.

First we detect harmonic motion with a sin-

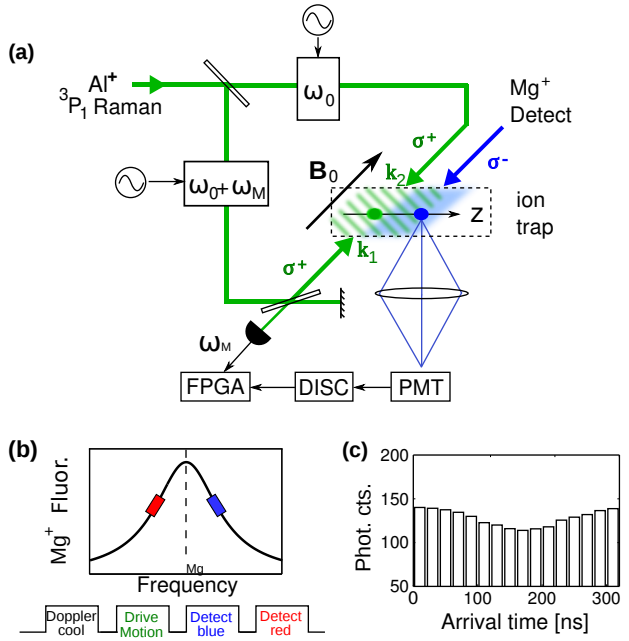

FIG. 1. (color online) (a) Experimental setup (DISC = discriminator, FPGA = field programmable gate array, PMT = photomultiplier tube). Counter–propagating Al^+ $^3P_1$ laser beams drive ion motion at their difference frequency ω_M, which is phase-stabilized with an interferometer near the ion trap. With a laser tuned near resonance, the Mg^+ ion scatters photons that are counted and time-binned with respect to the driving force in an FPGA. (b) During detection, the Mg^+ beam is tuned first above (blue) then below (red) the optical resonance, which amplifies then damps the motion respectively. Fluorescence from Mg^+ is modulated by the ion motion with the modulation phase shifted by π between the blue and red pulses. (c) Peak-to-peak fluorescence modulation of 20% when Al^+ in the $^1S_0$ state. In the $^3P_0$ state modulation is absent. The motional period of $2\pi/\omega_M = 340$ ns is divided into 16 photon-arrival-time bins.

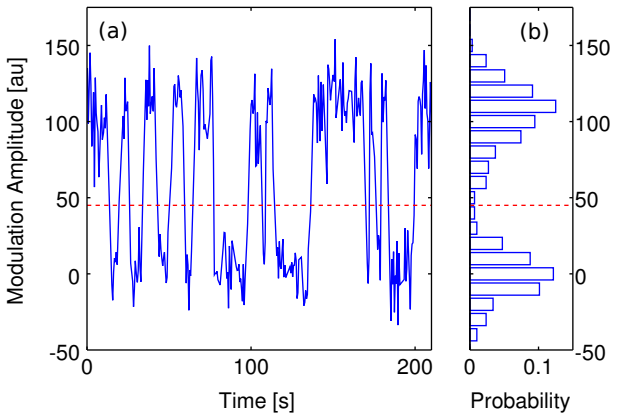

FIG. 2. (a) Steps in fluorescence modulation amplitudes corresponding to quantum jumps between the $^1S_0$ and $^3P_0$ clock states in Al^+, which are induced by a near-resonant laser beam or by spontaneous decay. The amplitude is extracted at the calibrated modulation phase and averaged over 0.53 s. (b) Histogram of mean modulation amplitudes from the entire data set. Dashed lines indicate the threshold for detecting transitions.

gle σ^--polarized Mg^+ detection beam, by observing modulation of the rate of photon scattering. The detection laser propagates in a direction anti-parallel to the magnetic field and is nearly resonant with the $|3s\,^2S_{1/2}, F = 3, m_F = -3\rangle \rightarrow |3p\,^2P_{3/2}, F = 4, m_F = -4\rangle$ cycling transition (frequency $\omega_{\rm Mg}$, linewidth $\Gamma_{\rm Mg} = 2\pi \times 41.4$ MHz). Photons scattered by this transition are collected with an overall efficiency of approximately 0.4 % on a photomultiplier tube. The excitation/detection sequence, depicted in Fig. 1(b), begins by laser cooling all normal modes to near the Doppler limit. Next, the optical drive of duration $t_d = 250\,\mu$s, applied to the Al^+ ion, excites the COM mode along the trap axis. Detection of the motion involves two sequential laser pulses of intensity 3 kW/m^2, the first tuned blue ($\omega_{\rm blue} \simeq \omega_{\rm Mg} + \Gamma_{\rm Mg}/2$) and the second red ($\omega_{\rm red} \simeq \omega_{\rm Mg} - \Gamma_{\rm Mg}/2$). Qualitatively, the blue-detuned pulse amplifies the motion, while the red-detuned pulse damps it [14]. The respective durations ($t_{\rm blue} = 400\,\mu$s, $t_{\rm red} = 200\,\mu$s) empirically maximize the detection signal. Fluorescence during both pulses is modulated at the frequency ω_M, albeit with a π phase shift that is compensated electronically.

The experimental signal is the modulation amplitude of the time-binned fluorescence at the calibrated frequency and phase of ion motion (Fig. 1(c)). We observe 20 % peak-to-peak modulation relative to the mean fluorescence when Al^+ is in the $^1S_0$ state. Figure 2(a) shows this signal as a function of time. Quantum jumps are visible, caused by periodic $^1S_0 \leftrightarrow {}^3P_0$ laser pulses, or by spontaneous decay from the $^3P_0$ state. The presence of modulation in the ion fluorescence corresponds to the Al^+ ion occupying the $^1S_0$ ground state, while its absence corresponds to the ion in the $^3P_0$ state, which has negligible interaction with the $^1S_0 \leftrightarrow {}^3P_1$ laser beams. Figure 2(b) shows a histogram of the modulation amplitude; these data reach 93 % state-detection fidelity within 80 ms. The detection rate could be improved by higher modulation amplitudes or photon collection efficiency.

A more sensitive method for distinguishing small amplitudes of motion uses resolved sideband transitions on the control ion. In this method, two hyperfine states of $^{25}Mg^+$ form a quantum bit $|\downarrow\rangle_{\rm Mg} \equiv |^2S_{\frac{1}{2}}, F = 3, m_F = -3\rangle$ and $|\uparrow\rangle_{\rm Mg} \equiv |^2S_{\frac{1}{2}}, F = 2, m_F = -2\rangle$ as described in previous work [15]. During a detection cycle, the ions are first cooled by stimulated-Raman transitions to near the ground state of motion [16] for the axial modes before applying the optical driving force. In a quantum mechan-

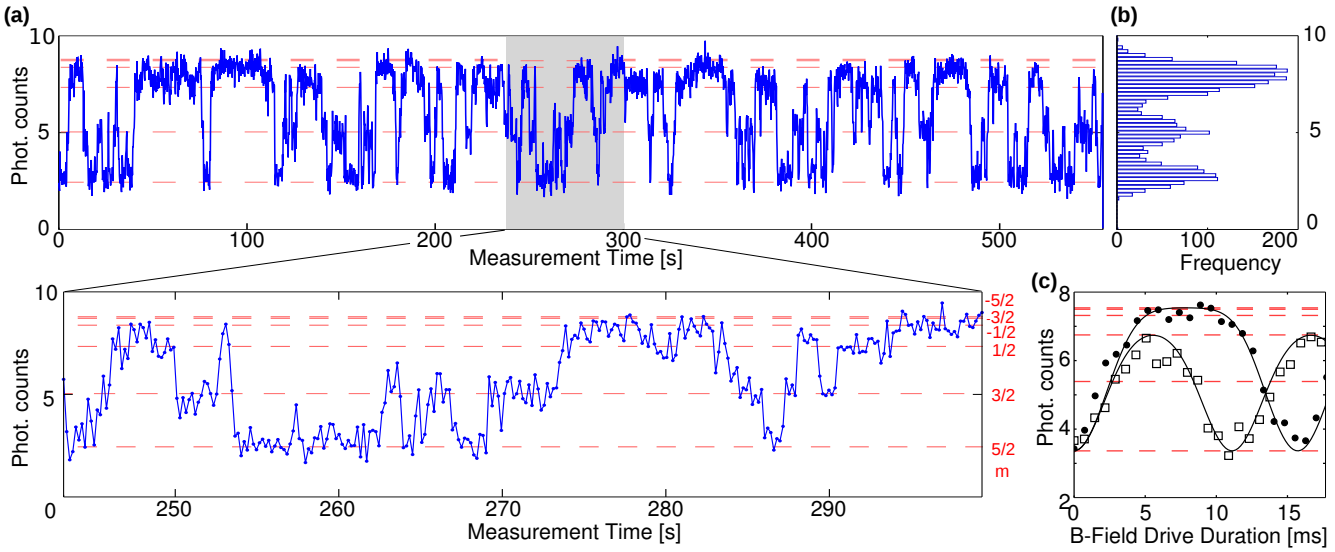

FIG. 3. (a) Quantum jumps between Zeeman substates of the $^1S_0$, $I = 5/2$ manifold in Al^+. Blue dots record the fluorescence levels in bins of 120 consecutive detections (1.6 ms detection duration). Red lines show predicted fluorescence levels based on the calibration for $m = +5/2$. *top* Several minutes of continuous detection. *bottom* A detailed view of 50 seconds of the detection data. (b) A histogram of the ion fluorescence signal (mean taken in bins of 120 experiments). (c) Magnetic resonance experiment an $^{27}Al^+$ ion initialized in the $^1S_0$, $m = 5/2$ state with $\Delta_B = 0$ (filled circles) and $\Delta_B = 2\Omega_B$ (open squares). The solid curves are calculations of fluorescence based on a fitted value of Ω_B, and an initial thermal motional mode with $\langle n\rangle = 0.15$. Red dashed lines show the expected detection fluorescence levels for different Zeeman states.

ical description, $\boldsymbol{F}^{(\mathrm{i})}(t)$ acting on an undamped oscillator displaces the ion motion in phase space by amplitude $\beta^{(\mathrm{i})} = F_0^{(\mathrm{i})} t_d z_{0,\mathrm{Al}}/2\hbar$ as described by the displacement operator $D(\beta^{(\mathrm{i})}) = \exp(\beta^{(\mathrm{i})} a^\dagger - \beta^{(\mathrm{i})*} a)$ [17]. Here a is the harmonic oscillator annihilation operator and $F_0^{(\mathrm{i})} \equiv \boldsymbol{F}_0^{(\mathrm{i})} \cdot \hat{\boldsymbol{z}}$ is the projection of the peak dipole force on the trap axis. When $D(\beta)$ acts on an initial ground state it produces a coherent state of motion $|\beta\rangle$. The probability distribution for $|\beta^{(\mathrm{i})}\rangle$ in terms of Fock states, $|n\rangle$, is $p^{(\mathrm{i})}(n) = e^{-|\beta^{(\mathrm{i})}|^2} |\beta^{(\mathrm{i})}|^{2n}/(n!)$. We probe this distribution with a red–sideband (RSB) pulse on the Mg^+ qubit transition [10]. Relaxation is negligible for typical pulse durations of 0 to 40 μs, and the $|\downarrow\rangle_{\mathrm{Mg}}$ state probability evolves as $P_\downarrow^{(\mathrm{i})}(t) = \sum_n p^{(\mathrm{i})}(n) \cos^2(\Omega_n t)$, where Ω_n is the RSB Rabi flopping rate for $|\downarrow\rangle_{\mathrm{Mg}}|n\rangle \rightarrow |\uparrow\rangle_{\mathrm{Mg}}|n-1\rangle$. By measuring $P_\downarrow$ for a particular duration t, we gain information about β to identify the current state $|i\rangle$.

To demonstrate this method, we experimentally distinguish Zeeman substates $|I, m\rangle$ of the Al^+ $^1S_0$ ground state, which has angular momentum $\hbar\boldsymbol{I}$ with $I = 5/2$ and magnetic moment $\boldsymbol{\mu} = g_I \mu_B \boldsymbol{I}$, where μ_B is the Bohr magneton and g_I is the nuclear g-factor [18] ($g_I = -0.00097248(14)$). The applied static magnetic field $\boldsymbol{B}_0$ gives rise to six Zeeman states $|I, m\rangle$ for $m = -5/2$ to $+5/2$ that are equally separated in energy by $\hbar\omega_{0B} = |g_I \mu_B B_0|$ in the absence of other perturbations. The coherent state amplitudes $\beta^{(m)}$ for the various Zeeman states depend on the Clebsch-Gordan coefficients, $\langle \frac{5}{2}, m; 1, 1 | \frac{7}{2}, m+1\rangle$, and the Raman detuning, $\Delta^{(m)} \equiv \Delta_R + g_{^3\mathrm{P}_1}(5/2 - m)\mu_B B_0$. Here, $g_{^3\mathrm{P}_1} \simeq 3/7$ is the $^3P_1$ $g-$factor, when nuclear and relativistic corrections are neglected. For small Al^+ motional amplitudes in the Lamb-Dicke limit ($\beta z_{0,\mathrm{Al}} \ll c/(\sqrt{2}\omega_L)$),

$$|\beta^{(m)}| = \eta \left(\Omega_0' \langle \frac{5}{2}, m; 1, 1 | \frac{7}{2}, m+1 \rangle \right)^2 t_d/|\Delta_m|, \qquad (1)$$

where Ω_0' is the carrier Rabi rate for the $|I, m = 5/2\rangle \rightarrow |^3\mathrm{P}_1, F = 7/2, m_F = 7/2\rangle$ transition. We calibrate Ω_0' by optically pumping to $|I, m = 5/2\rangle$, applying the optical drive pulse for duration t_d and scanning the duration of the Mg^+ RSB pulse [10]. We fit a coherent state amplitude $\beta^{(5/2)}$ to the resulting curve and calculate the other $\beta^{(m)}$ based on Eq. 1. In the experiment here, $\Omega_0'/2\pi = 0.85$ MHz and for $t_d = 50$ μs, $\{\beta^{(m)}\} = \{0.05, 0.16, 0.37, 0.71, 1.26, 2.15\}$, in order of increasing m. We choose $t_{\mathrm{rsb}} = 2.8$ μs to differentiate several of the Zeeman states.

In Fig. 3(a) we record quantum jumps of the fluorescence signal as a function of time when we repeatedly apply the detection procedure without state preparation. Each data point corresponds to the average photon counts from 120 consecutive detection cycles (1.6 ms cycle time). Several distinct fluorescence levels are visible, which agree with the above calibration. Jumps in the fluorescence level correspond to changes in the Zeeman state that occur during the measurement process. The jumps appear to be caused by polarization imperfection in the $^3P_1$ Raman beams. With residual π or σ^--polarization, a two-photon stimulated-Raman process can induce transitions between Zeeman states, and a laser field with 3 %

residual π-polarization would cause the observed rate of quantum jumps.

The tendency of the fluorescence to persist at a particular level indicates the nondestructive nature of the detection method. This is possible without a cycling transition for the Zeeman sublevels because the off-resonant laser pulses give only a small probability ($\approx 1 \times 10^{-4}$ for $m = 3/2$) of spontaneous-Raman scattering through the $^1S_0 \leftrightarrow {}^3P_1$ transition in a single detection cycle. In this regime, a histogram of averaged fluorescence levels (Fig. 3(b)) for the entire detection record will exhibit separate maxima in the distribution, which correspond to the resolvable states.

To further characterize this detection protocol, we perform a nuclear magnetic resonance experiment on the $^1S_0$ electronic ground state of $^{27}Al^+$. An oscillating magnetic field $B_1 \cos\omega_B t$ in a direction perpendicular to the static field $\boldsymbol{B}_0$ induces transitions between Zeeman states. Our case of small detuning ($\Delta_B \equiv \omega_B - \omega_{0B} \ll \omega_B$) and weak drive ($B_1 < B_0$), allows the rotating–wave approximation, where the angular momentum is affected primarily by the component of the oscillating field that rotates about $\boldsymbol{B}_0$ in the same sense as the Larmor precession of the magnetic dipole. More generally, the coupled Schrödinger equations determine the probability $P_{I,m}(t)$ of finding the ion in state $|I, m\rangle$.

We initialize Al^+ in $|I, m = 5/2\rangle$ and plot the fluorescence signal for different values of Δ_B as a function of the B-field modulation pulse duration (Fig. 3(c)). In the experiment $B_0 = 0.74$ mT ($\omega_{0B} \simeq 2\pi \times 8.3$ kHz). A fit to the data for zero detuning ($\Delta_B = 0$) yields the Rabi flopping rate Ω_B, and this value is used to calculate the curve for $\Delta_B = 2\Omega_B$ with no additional free parameters. Uncertainty associated with depumping during detection and imperfect ground state cooling affects the agreement between theory and experiment. For the theoretical curves shown here we use a residual (thermal) Fock state occupation of $\langle n \rangle = 0.15$ based on a separate calibration from sideband measurements after cooling.

In summary, we have explored a general method for detection of quantum states of trapped ions and have experimentally implemented two specific protocols to detect states in Al^+ by exciting state-dependent coherent motion. Although demonstrated on single ions, the same approach can be used to detect the states of multiple ions, and the optical driving force can be created in a variety of configurations with respect to laser frequencies, geometry, and polarization. As one practical application, the modulated fluorescence method can simplify Al^+ optical clocks [18] because lasers for ground-state cooling and resolved–sideband transitions are no longer needed. Technical improvements such as higher photon-collection efficiency and further optimised laser pulses can increase state-detection efficiency. Electromagnetically-induced transparancy (EIT) resonances [19] may also improve efficiency, because the reduced atomic line-width in this configuration enhances the velocity-sensitivity of the ion fluorescence.

On the other hand, the resolved–sideband method provides greater sensitivity to small amplitudes of motion that are generated by weak, non-destructive, interaction between the Stark-shifting lasers and the spectroscopy ion. Because internal state changes from spontaneous-Raman scattering can be suppressed, the present technique approaches the textbook ideal of a quantum measurement, where state collapse is the only effect. This provides a new route to perform spectroscopy on ion species where state changes from optical pumping are problematic. For example, the method might be used to detect ro-vibrational resonances in molecular ions [20, 21] by observing the magnitude and phase of coherent motion driven by far-off-resonant lasers.

We thank C. Oates for contributions to this work, and acknowledge support from AFOSR, DARPA, ONR and IARPA. Not subject to U.S. copyright.

* Present address: Kirchhoff-Institut für Physik, Universität Heidelberg, Im Neuenheimer Feld 227, 69120 Heidelberg, Germany; dhume@kip.uni-heidelberg.de

[1] R. Blatt and P. Zoller, Eur. J. Phys. **9**, 250 (1988).
[2] T. Basché, S. Kummer, and C. Bräuchle, Nature **373**, 132 (1995).
[3] S. Peil and G. Gabrielse, Phys. Rev. Lett. **83**, 1287 (1999).
[4] S. Gleyzes, et al., Nature **446**, 297 (2007).
[5] A. Lupascu, et al., Nat. Phys. **3**, 119 (2007).
[6] P. O. Schmidt, et al., in *Non-Neutral Plasma Physics VI*, edited by M. Drewsen and H. Knudsen (AIP, 2006) pp. 305 – 312.
[7] D. B. Hume, T. Rosenband, and D. J. Wineland, Phys. Rev. Lett. **99**, 120502 (2007).
[8] C. R. Clark, J. E. Goeders, Y. K. Dodia, C. R. Viteri, and K. R. Brown, Phys. Rev. A **81**, 043428 (Apr 2010).
[9] C. Monroe, D. M. Meekhof, B. E. King, and D. J. Wineland, Science **272**, 1131 (1996).
[10] D. M. Meekhof, C. Monroe, B. E. King, W. M. Itano, and D. J. Wineland, Phys. Rev. Lett. **76**, 1796 (1996).
[11] M. J. Biercuk, H. Uys, J. W. Britton, A. P. VanDevender, and J. J. Bollinger, Nat. Nano. **5**, 646 (2010).
[12] S. Knünz, et al., Phys. Rev. Lett. **105**, 013004 (2010).
[13] E. Träbert, A. Wolf, J. Linkemann, and X. Tordoir, J. Phys. B **32**, 537 (1999).
[14] K. Vahala, et al., Nat. Phys. **5**, 682 (2009).
[15] D. B. Hume, C. W. Chou, T. Rosenband, and D. J. Wineland, Phys. Rev. A **80**, 052302 (2009).
[16] C. Monroe, et al., Phys. Rev. Lett. **75**, 4011 (1995).
[17] P. Carruthers and M. Nieto, Am. J. Phys. **33**, 537 (1965).
[18] T. Rosenband, et al., Phys. Rev. Lett. **98**, 220801 (2007).
[19] C. Roos, et al., Phys. Rev. Lett. **85**, 5547 (2000).
[20] I. Vogelius, L. Madsen, and M. Drewsen, J. Phys. B **39**, S1259 (2006).
[21] J. C. J. Koelemeij, B. Roth, and S. Schiller, Phys. Rev. A **76**, 023413 (2007).